AIMS Mathematics, 11(5): 15008–15027.
DOI: 10.3934/math.2026617
Received: 09 February 2026
Revised: 04 May 2026
Accepted: 18 May 2026
Published: 28 May 2026

https://www.aimspress.com/journal/Math

Research article

Asymptotic distribution of fiber intersection counts in two-dimensional random fiber webs

Heuiju Chun[1] **and Jae-Hwan Jhong**[2,*]

[1] Department of Statistics and Information, Dongduk Women's University, 60, Hwarang-ro 13-gil, Seongbuk-gu, Seoul, 02748, Republic of Korea

[2] Department of Information Statistics, Chungbuk National University, 1, Chungdae-ro, Cheongju-si, Chungcheongbuk-do, 28644, Republic of Korea

* **Correspondence:** Email: jjh25@cbnu.ac.kr; Tel: +82432612256; Fax: +82432735928.

Abstract: We study the asymptotic distribution of the number of fiber intersections in two-dimensional random fiber webs. Previous work on such systems has focused primarily on first- and second-order moment characteristics derived from geometric probability models. In this paper, we move beyond moment-based analysis and establish asymptotic normality for normalized intersection counts. For a planar fiber web consisting of line segments randomly placed with uniform locations and orientations, we show that the appropriately normalized number of intersections within a bounded observation window converges in distribution to a Gaussian limit as the number of fibers diverges. We first derive a central limit theorem for the equal-length fiber model and then extend the result to heterogeneous fiber systems with a mixture of two fiber lengths. In both cases, explicit expressions for the asymptotic mean and variance are obtained in terms of the first two moments of the truncated fiber lengths within the counting region. Theoretical results are supported by Monte Carlo simulations, which demonstrate that the Gaussian approximation provides an accurate description of the finite-sample distribution of the intersection count. Our findings place random fiber intersection models within the broader framework of stochastic geometry and provide a foundation for statistical inference in fiber-based network systems.

Keywords: asymptotic normality; random fiber web; geometric probability; stochastic geometry; intersection count
Mathematics Subject Classification: 60D05, 62E20, 65C05

1. Introduction

Random fiber systems are widely used as canonical stochastic models for nonwoven materials, paper sheets, and fibrous composites. In such systems, fibers are often idealized as line segments randomly placed in a planar region with random locations and orientations, generating complex networks whose geometric characteristics are closely related to macroscopic properties such as strength, permeability, and connectivity. Among various descriptors, the number of fiber intersections is particularly important, as it directly reflects the degree of entanglement and connectivity of the fiber web.

Beyond their structural role, fiber intersection statistics are closely linked to a wide range of functional properties in fibrous materials. In nonwoven fabrics and paper sheets, intersection density has been shown to be strongly associated with basis weight nonuniformity, pore size distributions, and transport characteristics such as air and liquid permeability [1–3]. These geometric descriptors play a central role in filtration performance and flow resistance in fibrous media.

Fiber intersections are also known to influence acoustic absorption and sound transmission in fibrous materials, where the connectivity and tortuosity of the fiber network govern energy dissipation mechanisms. Experimental and modeling studies have demonstrated that microstructural features of random fiber networks, including intersection density and pore geometry, are key determinants of acoustic behavior in nonwoven and porous materials [4, 5]. From an engineering perspective, intersection statistics therefore provide an essential geometric bridge between microscopic fiber arrangements and macroscopic mechanical, filtration, and acoustic properties.

Probabilistic studies of fiber intersections trace back to classical geometric probability and stochastic geometry, where the primary emphasis has been on first- and second-order characteristics of intersection counts, typically under homogeneous and isotropic placement assumptions. Early work on idealized planar fiber networks includes the statistical geometry approach of [1] and related investigations accounting for crossings in two-dimensional assemblies [4, 6]. A later revisit emphasizing geometric features such as waviness, dimensionality, and percolation in random fibrous networks was provided by [5]. These works establish the foundational viewpoint that intersection statistics are central to understanding fibrous microstructures.

A systematic and analytically tractable framework for intersection counting in two-dimensional random fiber webs was developed in a series of papers by Chun and coauthors. In particular, Suh et al. [7] introduced a geometric probability model in which fibers are seeded in a seeding region, and intersections are counted within a counting region, enabling explicit treatment of boundary truncation (edge effects). Under an equal-length fiber model, they derived closed-form expressions for the expectation and variance of the intersection count and validated the resulting approximations through Monte Carlo simulation. Extending the probabilistic building blocks, Chun [8] studied the distribution of fiber length segments truncated by a bounded observation window, providing explicit formulas for the density and the first two moments of the effective length within the counting region—quantities that are essential inputs for second-order analyses of intersections. More recently, Chun and Suh [9] generalized the equal-length model to a two-component mixture of fiber lengths, substantially broadening applicability while preserving analytic tractability for the first two moments.

Despite these advances, existing studies on random fiber intersections have been largely confined to moment-based analyses. From a statistical perspective, however, distributional limit theory is

indispensable for uncertainty quantification and inferential procedures in large-scale fiber systems, as mean–variance characterizations alone do not provide asymptotic sampling distributions for normalized intersection counts. Addressing this gap is the main objective of the present paper.

We establish the asymptotic normality of the number of fiber intersections in two-dimensional random fiber webs for both the equal-length model and the two-length mixture model. Our starting point is the pairwise indicator representation of the intersection count as a sum over unordered fiber pairs, which induces a nontrivial dependency structure through shared fibers and boundary truncation. To handle this dependence, we exploit conditional independence properties inherent in the geometric construction together with sharp variance scaling. Conceptually, our setting is closely related to central limit theorems for dependent sums in stochastic geometry, including quantitative normal approximations for Poisson-based U-statistics [10] and limit theorems for stabilizing geometric functionals [11]. We also draw on standard tools from geometric probability [12–14] and modern stochastic analysis for Poisson processes [15, 16] to place the results in a broader methodological context.

The contributions of this paper can be summarized as follows. First, we provide a rigorous proof that the appropriately normalized intersection count converges in distribution to a standard normal law under a natural asymptotic regime in which the number of fibers diverges. Second, we extend the theory to heterogeneous webs with a two-length mixture, yielding a unified asymptotic framework that complements and generalizes the existing moment-based theories of [7] and [9]. Third, we support the theoretical findings with simulation studies, demonstrating that the normal approximation can be accurate in practically relevant finite-sample regimes.

The remainder of the paper is organized as follows. Section 2 introduces the random fiber web model and the geometric setup. Section 3.1 presents the main asymptotic normality result for the equal-length case, together with proofs. Section 3.2 extends the limit theory to the two-length mixture model. Section 4 reports simulation results assessing the finite-sample accuracy of the Gaussian approximation. Section 5 concludes with a discussion of implications and future directions.

2. Preliminaries

In this section, we review the geometric setup and notation for two-dimensional random fiber webs, largely following the framework established in [7–9]. The purpose of this section is to provide a unified description of the seeding and counting regions, fiber placement, and intersection indicators, which will be used throughout the subsequent asymptotic analysis.

2.1. Geometric setup: Seeding and counting regions

Let $C \subset \mathbb{R}^2$ denote a bounded planar region, referred to as the counting region, within which fiber intersections are observed. To properly account for boundary truncation effects, fibers are generated by seeding their midpoints in a larger region $S \supset C$, called the seeding region. The size of S is chosen so that any fiber whose midpoint lies in S may potentially intersect C.

Each fiber is represented by a straight line segment of fixed length l (or a random length, depending on the model), with its midpoint uniformly distributed over S and its orientation independently and uniformly distributed on $[0, \pi)$. This construction ensures stationarity and isotropy of the fiber process within C, while explicitly incorporating edge effects induced by the bounded observation window.

2.2. Truncated fiber length

Let L denote the random length of the portion of a fiber that lies within the counting region C. Even when all fibers have identical original length l, the random variable L is nondegenerate due to boundary truncation. The distribution of L and its expectation $\mathbb{E}(L)$ and variance $\mathrm{Var}(L)$ play a fundamental role in characterizing intersection probabilities and their second-order properties.

The exact distribution of L depends on the geometry of C and S and has been derived explicitly in [8]. In particular, for a fixed counting region C, both $\mathbb{E}(L)$ and $\mathrm{Var}(L)$ are finite constants that do not depend on the number of fibers. These quantities will appear repeatedly in the asymptotic expressions for the mean and variance of the intersection count.

2.3. Intersection indicators and dependence structure

Consider n fibers generated as described above. For each unordered pair of distinct fibers (i, j), define the intersection indicator

$$Y_{ij} = \begin{cases} 1, & \text{if fibers } i \text{ and } j \text{ intersect within } C, \\ 0, & \text{otherwise.} \end{cases}$$

The total number of fiber intersections within C is then given by

$$Y = \sum_{1 \le i < j \le n} \sum Y_{ij}.$$

Under the geometric probability model of [7], the probability that two fibers intersect within C is

$$\mathbb{P}(Y_{ij} = 1) = \frac{2\mathbb{E}(L)^2}{\pi |C|},$$

where $|C|$ denotes the area of the counting region. Consequently, the expectation of Y is of order n^2.

Although the indicators $\{Y_{ij}\}$ are identically distributed, they are not mutually independent. In particular, Y_{ij} and Y_{ik} are dependent due to the shared fiber i. This pairwise dependence induces a nontrivial dependency graph structure on the collection $\{Y_{ij}\}$, which is central to the asymptotic analysis carried out in this paper. Importantly, conditional on a given fiber, intersection events involving that fiber exhibit a form of conditional independence that can be exploited in variance calculations and limit theorems.

2.4. Extension to mixture models

In the mixture fiber model considered by [9], fibers are divided into two groups with lengths l_1 and l_2, with corresponding truncated lengths L_1 and L_2. Throughout this paper, we adopt the convention that both fiber types share a common seeding region $S \supset C$, so the intersection probability formulas used in the asymptotic analysis apply uniformly across fiber types. Intersection indicators are then defined separately for pairs of fibers within the same group and across different groups. The resulting total intersection count can again be expressed as a sum of Bernoulli-type indicators, with expectations and variances determined by $\mathbb{E}(L_1)$, $\mathbb{E}(L_2)$, $\mathrm{Var}(L_1)$, and $\mathrm{Var}(L_2)$.

The asymptotic normality results developed in subsequent sections apply to both the equal-length and mixture models under a unified framework, with differences arising only through these moment quantities.

2.5. Asymptotic regime

Throughout this paper, we consider an asymptotic regime in which the number of fibers diverges while the counting region C and the seeding region S remain fixed. Under this regime, the intersection count Y grows on the order of n^2, and appropriate normalization leads to nondegenerate Gaussian limits. All limit theorems are stated with respect to this asymptotic framework.

3. Asymptotic normality

3.1. Fibers of equal length

In this section, we establish the asymptotic normality of the number of fiber intersections for the equal-length fiber model. All fibers are assumed to have a common length l, and the geometric construction follows the setup described in Section 2.

Theorem 3.1 shows that the normalized intersection count $Y/\{n(n-1)\}$ converges in distribution to a Gaussian limit with mean μ and variance of order n^{-1}. In particular, although Y itself grows on the order of n^2, its relative fluctuation around the deterministic limit μ is of order $n^{-1/2}$. This result extends the moment-based theory of [7] by establishing a full distributional limit for the intersection count.

Theorem 3.1 (Asymptotic normality for equal-length fibers)**.** *Let Y denote the total number of fiber intersections within the counting region C generated by n fibers of equal length l. Assume that fibers are independently seeded with uniformly distributed midpoints over the seeding region $S \supset C$ and independent, uniformly distributed orientations on $[0, \pi)$.*

Let L denote the random truncated fiber length within C, and define

$$\mu = \frac{\mathbb{E}(L)^2}{\pi|C|}, \qquad \sigma^2 = \frac{4\mathbb{E}(L)^2 \operatorname{Var}(L)}{\pi^2|C|^2}.$$

Then, as $n \to \infty$,

$$\sqrt{n}\left(\frac{Y}{n(n-1)} - \mu\right) \xrightarrow{d} N(0, \sigma^2).$$

Equivalently,

$$\frac{\sqrt{n}}{\sigma}\left(\frac{Y}{n(n-1)} - \mu\right) \xrightarrow{d} N(0, 1).$$

Proof. The intersection count admits the U-statistic representation

$$Y = \binom{n}{2} U_n, \qquad U_n = \binom{n}{2}^{-1} \sum_{1 \le i < j \le n} h(\xi_i, \xi_j),$$

where $\xi_i = (m_i, \theta_i)$ is the independent andd identically distributed(i.i.d.) marker of fiber i, and $h(\xi_i, \xi_j) = Y_{ij}$ is the Bernoulli intersection indicator. Classifying covariances by the number $s \in \{0, 1, 2\}$ of shared fibers and conditioning on the shared fiber (Lemma A.1) gives

$$\operatorname{Var}(Y) = \binom{n}{2}\theta(1-\theta) + n(n-1)(n-2)\sigma^2, \qquad \theta = 2\mu = \frac{2\mathbb{E}(L)^2}{\pi|C|}$$

so that $\mathrm{Var}(Y/[n(n-1)]) = \sigma^2/n + O(n^{-2})$. The first-order Hoeffding projection of h,

$$h_1(\xi_1) = \mathbb{E}[h(\xi_1, \xi_2) \mid \xi_1] - \theta = \frac{2\mathbb{E}(L)}{\pi|C|}(L_1 - \mathbb{E}(L)),$$

has variance $\zeta_1 = \sigma^2 > 0$ whenever $S \supsetneq C$ (because then $\mathrm{Var}(L) > 0$). Applying Hoeffding's classical central limit theorem (CLT) for one-sample U-statistics [17, 18], whose integrability hypothesis $\mathbb{E}h^2 \leq 1$ is trivially met, yields $\sqrt{n}(U_n - \theta) \xrightarrow{d} N(0, 4\zeta_1)$ and supports the claim. Full details are given in Appendix A.2. □

The asymptotic normality established in Theorem 3.1 provides a robust theoretical foundation for statistical inference in fiber network analysis. Although previous studies primarily relied on moment-based estimation, the explicit derivation of the limiting distribution allows for the construction of confidence intervals and hypothesis testing for intersection counts in large-scale webs. In particular, as the number of fibers n increases, the complex local dependence structure averages out, and the aggregate count behaves as a Gaussian random variable at the $n^{-1/2}$ scale.

3.2. Mixture of two fiber lengths

We now extend the asymptotic normality result to a heterogeneous fiber web consisting of two types of fibers with different lengths. This setting follows the mixture model introduced in [9] and substantially broadens the applicability of the equal-length theory developed in the previous section. Throughout, we retain the common-seeding-region convention of Section 2: Both fiber types share the same seeding region S.

Theorem 3.2 establishes a Gaussian limit for the normalized intersection count in heterogeneous fiber webs. The limiting mean μ corresponds to a weighted combination of intersection probabilities across within-type and between-type fiber pairs, and the asymptotic variance σ^2 reflects both within-type variability and cross-type interactions. The result reduces to Theorem 3.1 when $l_1 = l_2$.

Theorem 3.2 (Asymptotic normality for a two-length mixture)**.** *Consider a random fiber web consisting of two groups of fibers with lengths l_1 and l_2, sharing a common seeding region S. Let n_1 and n_2 denote the numbers of fibers of lengths l_1 and l_2, respectively, and set $n = n_1 + n_2$. Assume*

$$\frac{n_1}{n} \to \lambda_1, \qquad \frac{n_2}{n} \to \lambda_2, \qquad \lambda_1 + \lambda_2 = 1, \quad \lambda_1, \lambda_2 \in (0, 1),$$

as $n \to \infty$.

Let L_1 and L_2 denote the truncated fiber lengths within the counting region C corresponding to original lengths l_1 and l_2, respectively. Define

$$\mu = \frac{1}{\pi|C|}(\lambda_1\mathbb{E}(L_1) + \lambda_2\mathbb{E}(L_2))^2,$$

and

$$\sigma^2 = \frac{4}{\pi^2|C|^2}(\lambda_1 \mathrm{Var}(L_1) + \lambda_2 \mathrm{Var}(L_2))(\lambda_1\mathbb{E}(L_1) + \lambda_2\mathbb{E}(L_2))^2.$$

Then, as $n \to \infty$,

$$\sqrt{n}\left(\frac{Y}{n^2} - \mu\right) \xrightarrow{d} N(0, \sigma^2),$$

where Y denotes the total number of fiber intersections within C.

Proof. Decompose $Y = Y^{(11)} + Y^{(12)} + Y^{(22)}$ into within-type and cross-type components. Each component is a Bernoulli U-statistic in the markers of the underlying i.i.d. samples; by Lemma A.1, $\mathbb{E}Y_{ij}^{(gg')} = 2\mathbb{E}(L_g)\mathbb{E}(L_{g'})/(\pi|C|)$, and the expectation formula follows. Classifying nonzero covariances between pairs of indicators by the number and type of shared fibers (see the table in Appendix A.3) yields six cases, whose total contribution factors as

$$n \cdot \mathrm{Var}(Y/n^2) \longrightarrow \sigma^2 = \frac{4(\lambda_1 \mathrm{Var}(L_1) + \lambda_2 \mathrm{Var}(L_2))(\lambda_1 \mathbb{E}(L_1) + \lambda_2 \mathbb{E}(L_2))^2}{\pi^2 |C|^2}.$$

Asymptotic normality then follows from the two-sample U-statistic CLT [18, 19]: The joint Hoeffding projection of $(Y^{(11)}, Y^{(12)}, Y^{(22)})$ onto the first-order components of the two samples yields a jointly Gaussian limit, so any fixed linear combination, in particular Y/n^2, is asymptotically Gaussian. Nondegeneracy of σ^2 follows from $\lambda_1 \mathrm{Var}(L_1) + \lambda_2 \mathrm{Var}(L_2) > 0$, which holds as soon as the truncated-length distribution of either type is nondegenerate. Full details, including the enumeration of the six covariance cases, are given in Appendix A.3. □

Remark 3.1. *The asymptotic variance contains* $\lambda_1 \mathrm{Var}(L_1) + \lambda_2 \mathrm{Var}(L_2)$ *but no covariance between* L_1 *and* L_2*. This is because* L_1 *and* L_2 *are the truncated lengths of* different *fibers, which are independent by construction;* $\mathrm{Cov}(L_1, L_2) = 0$ *trivially. Cross-type effects nonetheless enter* σ^2 *through the squared mean factor* $(\lambda_1 \mathbb{E}(L_1) + \lambda_2 \mathbb{E}(L_2))^2$*, whose expansion contributes the cross-mean* $2\lambda_1\lambda_2\mathbb{E}(L_1)\mathbb{E}(L_2)$*. The latter is precisely the contribution of the cross-type covariance cases* (11) ↔ (12) *and* (22) ↔ (12) *in the enumeration of Appendix A.3.*

Remark 3.2 (Extension to general fiber-length distributions)**.** *Sections 3.1 and 3.2 focus on the equal-length and two-length mixture models, but the structure of the proofs suggests that the asymptotic normality hinges primarily on (i) the pairwise indicator representation* $Y = \sum_{i<j} Y_{ij}$ *and (ii) the first two moments of the truncated length(s) within the counting region. Suppose each fiber has a random original length* ℓ *drawn i.i.d. from a distribution on* $(0, \infty)$*, and let* L *be the corresponding truncated length within* C*. If* $\mathbb{E}(L)$ *and* $\mathrm{Var}(L)$ *are finite, and the induced dependence among the intersection indicators remains "local" (i.e., nonzero covariances arise only through shared fibers, as in Section 2), then the same normalization as in Theorem 3.1 is expected to yield a Gaussian limit with* $\mu = \mathbb{E}(L)^2/(\pi|C|)$ *and* $\sigma^2 = 4\mathbb{E}(L)^2 \mathrm{Var}(L)/(\pi^2|C|^2)$*, up to higher-order terms. A further natural variant, suggested by a reviewer, is to allow* type-dependent seeding regions S_g *in the mixture model; this introduces an extra geometric factor in the cross-type intersection probability and leads to a qualitatively similar CLT, but we do not pursue it here. A rigorous treatment of both extensions would require additional technical conditions to control boundary truncation and the variance scaling, and we leave them as important topics for future work.*

4. Simulation study

This section empirically assesses the finite-sample accuracy of the Gaussian limits established in Theorems 3.1 and 3.2. We focus on the two-length mixture setting, as it contains the equal-length model as a special case and captures the heterogeneity commonly observed in practice.

Throughout the simulation, fibers of both types are seeded under the common seeding region convention used in the theoretical development: Midpoints are drawn independently and uniformly

from a single bounded set $S \supset C$, and orientations are drawn independently and uniformly from $[0, \pi)$. Concretely, for a counting region $C \subset [-L_{\max}, L_{\max}]^2$, we take S to be a square of side $(\operatorname{diam} C) + l_{\max}$ centered on C, where $l_{\max} = \max(l_1, l_2)$; this ensures that every fiber whose midpoint lies in S may potentially intersect C, and that the intersection probability formulas (A.11) of Appendix A.3 apply uniformly across fiber types.

4.1. Baseline configuration

Our baseline configuration takes a square counting region C of side length 100 (so $|C| = 10{,}000$) and a two-type fiber web with $n = 1000$ fibers, consisting of $n_1 = 600$ fibers of length $l_1 = 10$ and $n_2 = 400$ fibers of length $l_2 = 30$. Figure 1 illustrates a single realization. The square corresponds to the counting region C, within which fiber intersections are recorded; line segments represent fibers seeded over S with independent uniform orientations. Fibers of different lengths are overlaid in the same spatial domain, resulting in a heterogeneous web with substantial overlap and interaction.

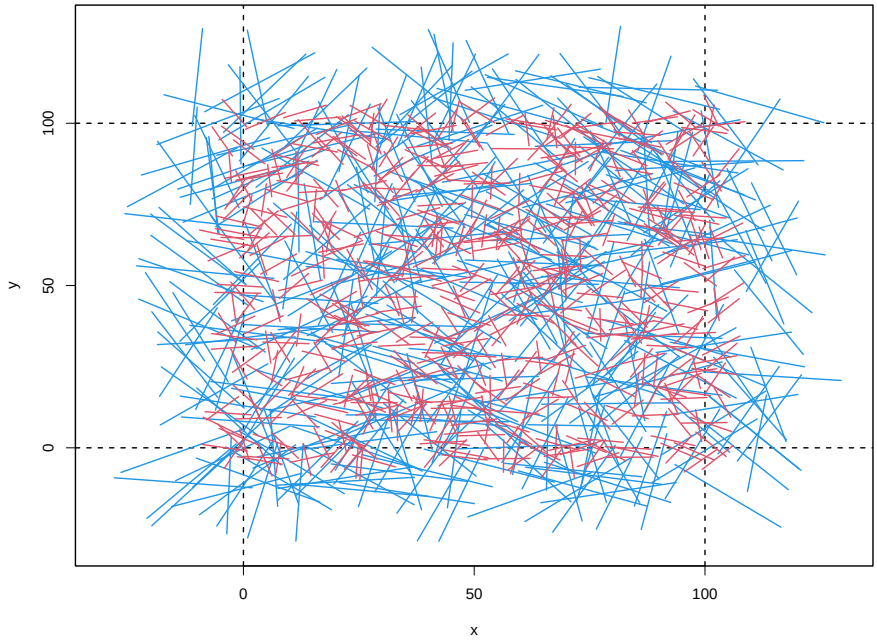

Figure 1. A single simulated realization of a two-dimensional random fiber web with two fiber lengths within the counting region C.

For each Monte Carlo replicate $r = 1, \ldots, R$ with $R = 1000$, we compute the total number of intersections $Y^{(r)}$ occurring within C and summarize the empirical distribution of $\{Y^{(r)}\}_{r=1}^{R}$. We compare it with (i) the theoretical mean and variance derived from the moment formulas underlying Theorem 3.2, and (ii) the asymptotic normal approximation implied by Theorem 3.2.

Let $\hat{m}_{\text{sim}}$ and $\hat{v}_{\text{sim}}$ denote the Monte Carlo mean and variance of Y based on $\{Y^{(r)}\}_{r=1}^{R}$. Let $(m_{\text{th}}, v_{\text{th}})$ be the corresponding exact finite-n theoretical mean and variance implied by Eq (A.12) of Appendix A.3: m_{th} aggregates the three pairwise intersection probabilities, and v_{th} combines the Bernoulli diagonal term of order n^2 with the six covariance contributions of order n^3. Finally, let $v_{\text{AN}} = n^3\sigma^2$ be the

leading asymptotic variance predicted by Theorem 3.2; the asymptotic normal approximation is then $N(m_{\mathrm{AN}}, v_{\mathrm{AN}})$ with $m_{\mathrm{AN}} = n^2\mu$.

Table 1 reports these quantities together with quartiles of the simulated intersection counts. The empirical and exact finite-n theoretical values agree to within Monte Carlo error ($\hat{m}_{\mathrm{sim}}/m_{\mathrm{th}} - 1 < 0.8\%$ and $\hat{v}_{\mathrm{sim}}/v_{\mathrm{th}} - 1 \approx 1.3\%$), and the leading asymptotic variance v_{AN} is slightly smaller than v_{th}, reflecting the $O(n^2)$ Bernoulli diagonal correction that vanishes as $n \to \infty$.

Table 1. Simulation results for the two-length mixture baseline with $n = 1000$ fibers ($n_1 = 600$, $l_1 = 10$; $n_2 = 400$, $l_2 = 30$; square C of side 100) under the common seeding region convention. "Simulation" reports Monte Carlo estimates over $R = 1000$ replicates; "Exact (finite-n)" reports the exact theoretical mean and variance derived in Appendix A.3; and "Asy. normal" reports the leading asymptotic approximation $N(n^2\mu, n^3\sigma^2)$ implied by Theorem 3.2.

	Simulation	Exact (finite-n)	Asy. normal
mean	3590.7	3617.3	3617.3
1Q	3456.8	–	3486.3
median	3592.0	–	3617.3
3Q	3725.0	–	3748.4
variance	37688.2	37188.0	33900.3

Figure 2 compares the Monte Carlo histogram of Y to the asymptotic normal density implied by Theorem 3.2. The vertical reference lines indicate the Monte Carlo mean and the exact finite-n theoretical mean. The close alignment between these reference lines confirms the accuracy of the moment-based theory, and the overall agreement between the histogram and the asymptotic curve illustrates that the Gaussian approximation captures both the center and spread of the finite-sample distribution well, even at moderate n.

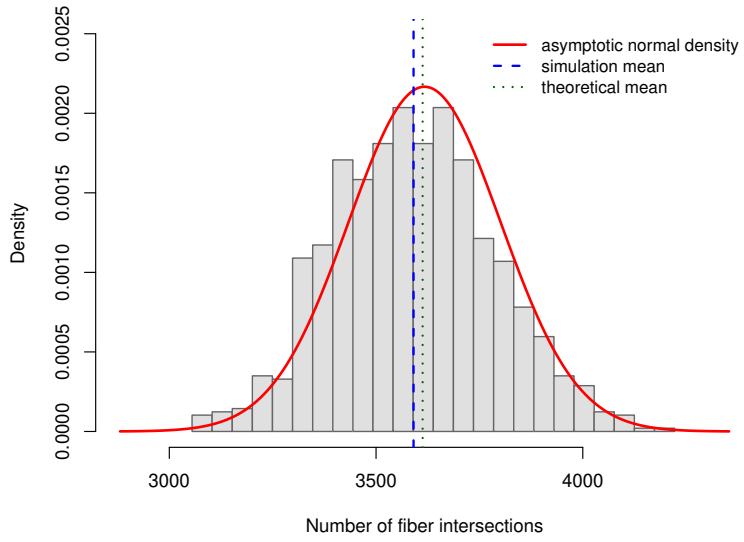

Figure 2. Empirical distribution of the intersection count Y under the two-length mixture baseline, compared with the asymptotic normal approximation $N(n^2\mu, n^3\sigma^2)$ implied by Theorem 3.2.

4.2. Convergence with respect to n

To verify the n^{-1} scaling of $\mathrm{Var}(Y/n^2)$ predicted by Theorem 3.2, we fix $(\lambda_1, l_1, l_2) = (0.6, 10, 30)$ and the square counting region of side 100, and vary n over $\{100, 200, 500, 1000, 2000\}$. For each n, we draw $R = 1000$ Monte Carlo replicates and compute the empirical slope $n \cdot \widehat{\mathrm{Var}}(Y/n^2)$, which Theorem 3.2 predicts to converge to $\sigma^2 \approx 3.38 \times 10^{-5}$.

Table 2 and Figure 3 show a clean monotone convergence: The empirical slope decreases from 6.94×10^{-5} at $n = 100$ to 3.46×10^{-5} at $n = 2000$, within 2.4% of the theoretical σ^2. The remaining gap is explained by the Bernoulli diagonal correction of order n^{-1} and is quantitatively captured by the exact finite-n variance formula from Appendix A.3.

Table 2. Convergence of empirical slope $n \cdot \widehat{\mathrm{Var}}(Y/n^2)$ to the asymptotic variance $\sigma^2 \approx 3.38 \times 10^{-5}$ as n increases. Configuration: $\lambda_1 = 0.6$, $l_1 = 10$, $l_2 = 30$, square C of side 100, common seeding region, $R = 1000$ replicates.

n	$\hat{m}_{\mathrm{sim}}$	$\hat{v}_{\mathrm{sim}}$	$n \cdot \widehat{\mathrm{Var}}(Y/n^2)$ $(\times 10^{-5})$
100	35.6	69.4	6.94
200	142.6	428.4	5.35
500	899.4	4757.5	3.81
1000	3619.5	37065.5	3.71
2000	14456.5	276904.1	3.46

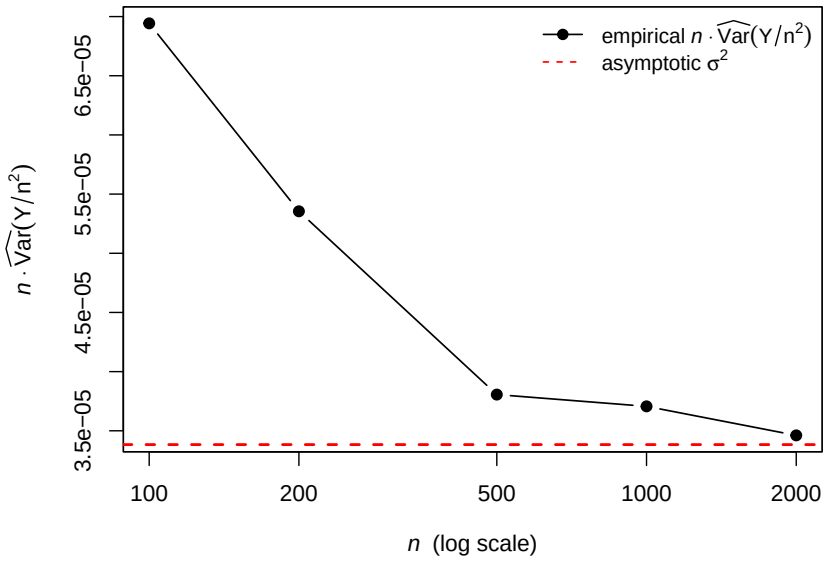

Figure 3. Empirical slope $n \cdot \widehat{\mathrm{Var}}(Y/n^2)$ versus the asymptotic variance σ^2 (red dashed line) as n increases. The slope is evaluated from $R = 1000$ Monte Carlo replicates at each n, with $\lambda_1 = 0.6$, $l_1 = 10$, $l_2 = 30$, and a square counting region of side 100.

4.3. Robustness to the shape of C

To investigate robustness to the geometry of the counting region, we fix $n = 1000$, $(n_1, n_2) = (600, 400)$, $l_1 = 10$, $l_2 = 30$, and consider three different shapes of C with the same area $|C| = 10{,}000$:

a square of side 100, a disk of radius $r = \sqrt{10{,}000/\pi} \approx 56.4$, and a rectangle 200×50. In each case, the common seeding region S is taken to be the corresponding dilation of C by $l_{\max}/2 = 15$.

The results are summarized in Table 3 and Figure 4. The empirical mean matches the exact finite-n theoretical mean within 1% for all three shapes; the empirical variance is within 1.4% of the full finite-n theoretical variance in each case. The asymptotic normal approximation (red curve in Figure 4) captures the bulk of the histogram well across shapes. The elongated rectangle exhibits a slightly larger empirical spread, consistent with the larger $\mathrm{Var}(L)/\mathbb{E}(L)^2$ produced by a more anisotropic counting region (cf. Remark A.1).

Table 3. Effect of counting-region shape on the simulation statistics. In each case, $n = 1000$, $(n_1, n_2) = (600, 400)$, $l_1 = 10$, $l_2 = 30$, and $|C| = 10{,}000$. Here, $v_{\mathrm{th}}^{\mathrm{exact}}$ denotes the exact finite-n theoretical variance from Appendix A Eq (A.12), and $v_{\mathrm{th}}^{\mathrm{AN}} = n^3\sigma^2$ denotes the leading asymptotic variance implied by Theorem 3.2.

Shape	$\hat{m}_{\mathrm{sim}}$	m_{th}	$\hat{v}_{\mathrm{sim}}$	$v_{\mathrm{th}}^{\mathrm{exact}}$	$v_{\mathrm{th}}^{\mathrm{AN}}$
square	3590.7	3617.3	37688.2	37325.9	33900.3
disk	2478.1	2499.4	27790.4	29079.6	26718.2
rectangle	3050.0	3037.8	32504.3	30820.4	27935.6

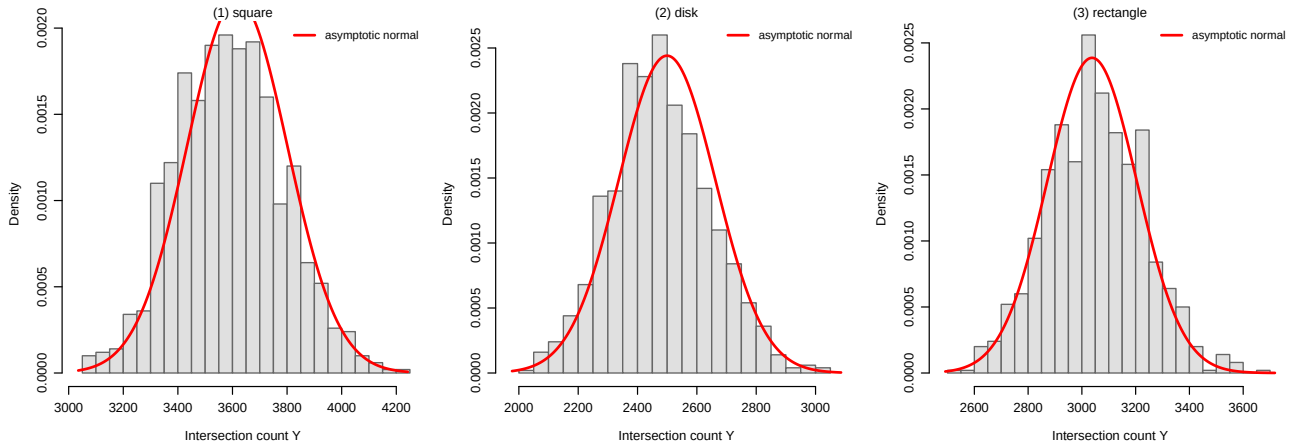

Figure 4. Empirical distribution of Y for three shapes of the counting region C with common area 10,000: square 100×100 (left), disk of radius $\sqrt{10{,}000/\pi}$ (middle), and rectangle 200×50 (right). Red curves are the asymptotic normal densities implied by Theorem 3.2.

4.4. Robustness to the mixing proportion λ_1

Finally, we fix the square counting region of side 100, $n = 1000$, and $(l_1, l_2) = (10, 30)$, and we vary the mixing proportion $\lambda_1 \in \{0.2, 0.5, 0.8\}$. Table 4 and Figure 5 show that both $\hat{m}_{\mathrm{sim}}$ and $\hat{v}_{\mathrm{sim}}$ track the theoretical values across the three regimes; the asymptotic normal approximation is adequate throughout, with the most visible departure occurring at $\lambda_1 = 0.8$, where the majority of fibers are short (length 10), and the intersection count is smaller, so that the finite-sample Edgeworth correction is still discernible.

Table 4. Effect of mixing proportion λ_1 on the simulation statistics. In each case, $n = 1000$, square C of side 100, $l_1 = 10$, $l_2 = 30$. Here, $v_{\text{th}}^{\text{exact}}$ denotes the exact finite-n theoretical variance from Appendix A Eq (A.12), and $v_{\text{th}}^{\text{AN}} = n^3\sigma^2$ denotes the leading asymptotic variance implied by Theorem 3.2.

λ_1	$\hat{m}_{\text{sim}}$	m_{th}	$\hat{v}_{\text{sim}}$	$v_{\text{th}}^{\text{exact}}$	$v_{\text{th}}^{\text{AN}}$
0.2	7531.0	7538.2	133320.3	127917.1	120927.8
0.5	4464.7	4464.5	49653.4	53576.1	49376.5
0.8	2178.9	2191.2	15065.0	15428.5	13317.8

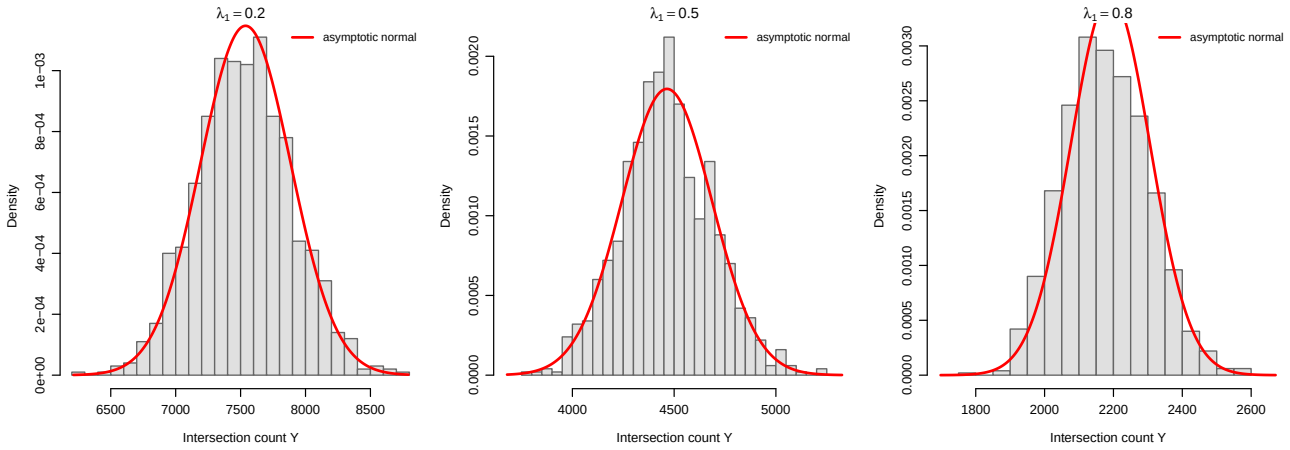

Figure 5. Empirical distribution of Y for three mixing proportions $\lambda_1 \in \{0.2, 0.5, 0.8\}$. Red curves are the asymptotic normal densities implied by Theorem 3.2.

Taken together, the simulation results provide strong empirical support for the asymptotic normality established in Theorems 3.1 and 3.2. The n^{-1} scaling of $\text{Var}(Y/n^2)$ is confirmed numerically, the Gaussian approximation is robust to the geometry of the counting region and to the mixing proportion λ_1, and the exact finite-n variance formula from Appendix A.3 accounts quantitatively for the small residual gap between the empirical and leading-order asymptotic variances.

5. Conclusions

This paper established the asymptotic normality of the number of fiber intersections in two-dimensional random fiber webs. Building on the geometric probability framework developed in earlier studies, we moved beyond moment-based characterizations and derived full distributional limits for normalized intersection counts.

For the equal-length fiber model, we showed that the appropriately normalized intersection count converges in distribution to a Gaussian limit, with explicit expressions for the asymptotic mean and variance determined by the first two moments of the truncated fiber length within the counting region. We then extended this result to heterogeneous fiber systems consisting of a mixture of two fiber lengths, demonstrating that asymptotic normality persists under a natural scaling regime when the proportions of different fiber types stabilize. In both settings, the key analytical challenge arises from the dependence structure induced by shared fibers and boundary truncation. Our results show that,

despite this dependence, the aggregation of a large number of weakly dependent pairwise intersection indicators leads to Gaussian fluctuations.

The simulation study corroborated the theoretical findings by illustrating that the asymptotic normal approximation provides an accurate description of the finite-sample distribution of the intersection count, even for moderately large numbers of fibers. Both the empirical mean and variance were well approximated by their theoretical counterparts, and the overall shape of the sampling distribution was closely captured by the Gaussian limit.

From a broader perspective, the results of this paper place random fiber intersection models within the growing body of stochastic-geometry problems for which central limit theorems can be established despite nontrivial local dependence. The explicit nature of the asymptotic mean and variance further enhances the practical usefulness of the theory, enabling uncertainty quantification and inferential procedures for fiber-based materials and related network models.

Several directions for future research remain open. One natural extension is to allow for more general fiber-length distributions, beyond the equal-length and two-component mixture models considered here. Another promising direction is to investigate asymptotic normality under alternative asymptotic regimes, such as simultaneous growth of the observation window and the number of fibers. Extensions to three-dimensional fiber systems and to models incorporating curvature or spatial inhomogeneity also merit further investigation. More broadly, the limit-theory framework employed here resonates with recent developments in adjacent application areas where distributional analysis of complex aggregate quantities plays a central role, including degradation modeling under heterogeneity [20] and complex survival data analysis incorporating clustering, cure fractions, and competing risks [21]. We hope that the results presented in this paper provide a foundation for such developments.

Author contributions

Heuiju Chun: Conceptualization, formal analysis and investigation, software and numerical simulation, writing—original draft preparation; Jae-Hwan Jhong: Methodology, formal analysis and investigation, software and numerical simulation, writing—review and editing. All authors have read and approved the final version of the manuscript for publication.

Use of Generative-AI tools declaration

The authors declare that they have not used Artificial Intelligence (AI) tools in the creation of this article.

Acknowledgments

This research was supported by the Global-Learning & Academic research institution for Master's·PhD students, and Postdocs (LAMP) Program of the National Research Foundation of Korea (NRF) grant funded by the Ministry of Education (No. RS-2024-00445180). The work of Jae-Hwan Jhong was supported by the National Research Foundation of Korea (NRF) grant funded by the Korea government (MSIT) (RS-2024-00342014).

Conflict of interest

The authors declare no conflict of interest.

References

1. O. Kallmes, H. Corte, The structure of paper. I. The statistical geometry of an ideal two dimensional fiber network, *Tappi J.*, **43** (1960), 737–752.
2. H. W. Piekaar, L. A. Clarenburg, Aerosol filters—Pore size distribution in fibrous filters, *Chem. Eng. Sci.*, **22** (1967), 1399–1407. https://doi.org/10.1016/0009-2509(67)80068-X
3. A. Rawal, S. Lomov, T. Ngo, I. Verpoest, J. Vankerrebrouck, Mechanical behavior of thru-air bonded nonwoven structures, *Text. Res. J.*, **77** (2007), 417–431. https://doi.org/10.1177/0040517507081313
4. T. Komori, Y. Ujihara, Y. Matsunaga, K. Makishima, Crossings of curled fibers in two-dimensional assemblies, *Tappi*, **62** (1979), 93–95.
5. Y. B. Yi, L. Berhan, A. M. Sastry, Statistical geometry of random fibrous networks, revisited: Waviness, dimensionality, and percolation, *J. Appl. Phys.*, **96** (2004), 1318–1327. https://doi.org/10.1063/1.1763240
6. J. H. Williams, S. S. Lee, C. S. Wasserman, Fiber intersections in a planar randomly oriented fiber composite, *Fibre Sci. Technol.*, **10** (1977), 161–177. https://doi.org/10.1016/0015-0568(77)90018-5
7. M. W. Suh, H. Chun, R. L. Berger, P. Bloomfield, Distribution of fiber intersections in two-dimensional random fiber webs – A basic geometrical probability model, *Text. Res. J.*, **80** (2010), 301–311. https://doi.org/10.1177/0040517509105071
8. H. Chun, Probabilistic modeling of fiber length segments within a bounded area of two-dimensional fiber webs, *Commun. Stat. Appl. Methods*, **18** (2011), 301–317.
9. H. Chun, M. W. Suh, Distribution of fiber intersections in two-dimensional random fiber web cases with a mixture of two fiber lengths, *Text. Res. J.*, **90** (2020), 1851–1859. https://doi.org/10.1177/0040517519898158
10. M. Reitzner, M. Schulte, Central limit theorems for u-statistics of poisson point processes, *Ann. Probab.*, **41** (2013), 3879–3909. https://doi.org/10.1214/12-AOP817
11. M. D. Penrose, J. E. Yukich, Central limit theorems for some graphs in computational geometry, *Ann. Appl. Probab.*, **11** (2001), 1005–1041.
12. M. G. Kendall, P. A. P. Moran, *Geometrical probability*, Hafner Publishing Company, 1963.
13. D. A. Klain, G. C. Rota, *Introduction to geometric probability*, Cambridge: Cambridge University Press, 1997.
14. H. Solomon, *Geometric probability*, 1978.
15. G. Last, M. D. Penrose, Poisson process Fock space representation, chaos expansion and covariance inequalities, *Probab. Theory Relat. Fields*, **150** (2011), 663–690. https://doi.org/10.1007/s00440-010-0288-5

16. G. Peccati, M. Reitzner, *Stochastic analysis for Poisson point processes: Malliavin calculus, wiener-Itô chaos expansions and stochastic geometry*, Springer, 2016.

17. W. Hoeffding, A class of statistics with asymptotically normal distribution, In: *Breakthroughs in statistics*, New York: Springer, 308–334. https://doi.org/10.1007/978-1-4612-0919-5_20

18. A. J. Lee, *U-Statistics: Theory and practice*, 1990. https://doi.org/10.1201/9780203734520

19. P. K. Sen, Almost sure convergence of generalized U-statistics, *Ann. Probab.*, **5** (1977), 287–290.

20. L. Zhuang, Y. Ma, G. Fang, A. Xu, Modeling two-scale degradation with heterogeneity: A unified random-effects inverse Gaussian framework, *IISE Trans.*, 2026. https://doi.org/10.1080/24725854.2026.2631614

21. Y. Wang, J. Li, Q. Zhou, W. Wang, A unified framework for complex survival data: accounting for clustering, cure fractions, and competing risks, *BMC Med. Res. Methodol.*, **26** (2026), 105. https://doi.org/10.1186/s12874-026-02842-z

Supplementary

A. Proofs of Theorems 3.1 and 3.2

Throughout this appendix, we adopt a common seeding region: All fibers (regardless of length) have midpoints drawn independently and uniformly from a single bounded set $S \supset C$, with orientations drawn independently and uniformly from $[0, \pi)$. This convention, inherited from [7] and [9], keeps the intersection probability formulas internally consistent across fiber types; cf. the discussion in Section 2.

Our main analytical tool is that the intersection count Y admits a U-statistic representation with a Bernoulli kernel. The asymptotic normality then follows from classical results for U-statistics [17, 18], once we verify the nondegeneracy of the associated Hoeffding projection.

A.1. Auxiliary lemma: Conditional intersection probability

We first record a conditional version of the intersection probability, which is the central ingredient of every covariance computation below.

Lemma A.1 (Conditional intersection probability)**.** *Let fiber i have an arbitrary but fixed midpoint $m_i \in S$ and orientation $\theta_i \in [0, \pi)$, and write L_i for the length of the portion of fiber i lying inside C. Let fiber j be independently generated with midpoint uniform in S, orientation uniform in $[0, \pi)$, and (possibly random) original length l_j with truncated length L_j. Then,*

$$\mathbb{P}\Big(Y_{ij} = 1 \,\Big|\, L_i, L_j \text{ distributions}\Big) \;=\; \mathbb{E}\Big[\mathbb{P}(Y_{ij} = 1 \mid L_i = \ell)\Big], \qquad \mathbb{P}(Y_{ij} = 1 \mid L_i = \ell) \;=\; \frac{2\,\ell\,\mathbb{E}(L_j)}{\pi|C|}. \tag{A.1}$$

In particular, in the equal-length setting $L_j \overset{d}{=} L_i$ and (A.1) *give $\mathbb{P}(Y_{ij} = 1) = 2\mathbb{E}(L)^2/(\pi|C|)$ after averaging over L_i.*

Proof. Fix fiber i as a line segment of truncated length ℓ inside C. Integrating the indicator that fiber j crosses this segment over $m_j \in S$ and $\theta_j \in [0, \pi)$ using the kinematic/Cauchy formula for line segments [7, 13, 14] yields a crossing probability that is linear in ℓ and in the expected truncated

length of the partner fiber, namely $2\ell\,\mathbb{E}(L_j)/(\pi|C|)$. Averaging over the distribution of L_i recovers the unconditional probability. Full details appear in [7, 8]. □

Equation (A.1) is what drives the local dependence structure of the indicators $\{Y_{ij}\}$: Conditional on the marker of one fiber, the indicators involving that fiber have conditional means that are *linear* in its truncated length. This is the only property of the geometry that we use in the following.

A.2. Proof of Theorem 3.1

Write $\xi_i = (m_i, \theta_i)$ for the marker of fiber i; the ξ_i's are i.i.d. by construction. Define the symmetric Bernoulli kernel

$$h(\xi_i, \xi_j) \;=\; \mathbf{1}\{\text{fibers } i \text{ and } j \text{ intersect within } C\} \;=\; Y_{ij}.$$

Then

$$Y \;=\; \sum_{1\le i<j\le n} h(\xi_i,\xi_j) \;=\; \binom{n}{2} U_n, \qquad U_n \;:=\; \binom{n}{2}^{-1} \sum_{i<j} h(\xi_i,\xi_j), \tag{A.2}$$

so that U_n is a (one-sample) U-statistic of order 2 with bounded kernel $h \in \{0, 1\}$. In particular, $\mathbb{E}\,h^2 \le 1 < \infty$, so the standard integrability hypothesis of Hoeffding's CLT is met.

Step 1. Hoeffding decomposition. Set $\theta := \mathbb{E}h(\xi_1, \xi_2)$, and define the first-order projection

$$h_1(\xi_1) \;:=\; \mathbb{E}[h(\xi_1,\xi_2)\,|\,\xi_1] - \theta. \tag{A.3}$$

By Lemma A.1,

$$\mathbb{E}[h(\xi_1,\xi_2)\,|\,\xi_1] \;=\; \frac{2L_1\mathbb{E}(L)}{\pi|C|}, \qquad \theta \;=\; \frac{2\mathbb{E}(L)^2}{\pi|C|}, \tag{A.4}$$

where $L_1 = L_1(\xi_1)$ is the truncated length of fiber 1. Hence,

$$h_1(\xi_1) \;=\; \frac{2\mathbb{E}(L)}{\pi|C|}(L_1 - \mathbb{E}(L)),$$

and

$$\zeta_1 \;:=\; \mathrm{Var}(h_1(\xi_1)) \;=\; \frac{4\mathbb{E}(L)^2}{\pi^2|C|^2}\,\mathrm{Var}(L) \;=\; \sigma^2. \tag{A.5}$$

The corresponding second-order kernel variance $\zeta_2 := \mathrm{Var}(h(\xi_1, \xi_2)) = \theta(1 - \theta) \le 1$ is finite.

Step 2. Variance of Y by number of shared fibers. We expand

$$\mathrm{Var}(Y) \;=\; \sum_{\{i,j\}}\sum_{\{k,l\}} \mathrm{Cov}(Y_{ij}, Y_{kl}), \tag{A.6}$$

and classify the pairs of pairs $(\{i, j\}, \{k, l\})$ by $s := |\{i, j\} \cap \{k, l\}| \in \{0, 1, 2\}$.

Case $s = 2$ (identical pair). There are $\binom{n}{2}$ such terms, each contributing $\mathrm{Var}(Y_{12}) = \theta(1 - \theta)$:

$$\Sigma_2 \;=\; \binom{n}{2}\theta(1-\theta).$$

Case $s = 1$ (one shared fiber). Ordered pairs $(\{i, j\}, \{k, l\})$ with exactly one common index: Pick the shared index (n ways), then two distinct partners ($(n-1)(n-2)$ ways), giving $n(n-1)(n-2)$ such ordered pairs. For any such pair, by symmetry,

$$\mathrm{Cov}(Y_{12}, Y_{13}) \;=\; \mathbb{E}[Y_{12}Y_{13}] - \theta^2. \tag{A.7}$$

Conditioning on ξ_1 and using that ξ_2, ξ_3 are i.i.d. given ξ_1,

$$\mathbb{E}[Y_{12}Y_{13} \,|\, \xi_1] \;=\; \mathbb{E}[Y_{12} \mid \xi_1]^2 \;=\; \left(\frac{2L_1\mathbb{E}(L)}{\pi|C|}\right)^2.$$

Taking expectations,

$$\mathbb{E}[Y_{12}Y_{13}] \;=\; \frac{4\mathbb{E}(L)^2\mathbb{E}(L^2)}{\pi^2|C|^2}, \qquad \mathrm{Cov}(Y_{12}, Y_{13}) \;=\; \frac{4\mathbb{E}(L)^2}{\pi^2|C|^2}(\mathbb{E}(L^2) - \mathbb{E}(L)^2) \;=\; \sigma^2.$$

Summing,

$$\Sigma_1 \;=\; n(n-1)(n-2)\,\sigma^2.$$

Case $s = 0$ (no shared fiber). The marker pairs (ξ_i, ξ_j) and (ξ_k, ξ_l) are then independent, so $\mathrm{Cov}(Y_{ij}, Y_{kl}) = 0$, and $\Sigma_0 = 0$.

Combining the three cases gives the exact variance

$$\mathrm{Var}(Y) \;=\; \binom{n}{2}\theta(1-\theta) \;+\; n(n-1)(n-2)\,\sigma^2. \tag{A.8}$$

This recovers (and corrects a minor typographical issue in) the expression reported in [7].

Step 3. Asymptotics and application of Hoeffding's CLT. Dividing (A.8) by $[n(n-1)]^2$,

$$\mathrm{Var}\left(\frac{Y}{n(n-1)}\right) \;=\; \frac{\theta(1-\theta)}{2n(n-1)} \;+\; \frac{(n-2)\,\sigma^2}{n(n-1)} \;=\; \frac{\sigma^2}{n} + O\left(\frac{1}{n^2}\right),$$

confirming $n\ \mathrm{Var}(Y/[n(n-1)]) \to \sigma^2$ as $n \to \infty$.

To obtain the limiting distribution, we invoke Hoeffding's theorem for one-sample U-statistics of order 2 (see, e.g., [18, Ch. 3]; original in [17]): If $\mathbb{E}h^2 < \infty$, and $\zeta_1 > 0$, then

$$\sqrt{n}\,(U_n - \theta) \;\xrightarrow{d}\; N(0, 4\zeta_1). \tag{A.9}$$

Verification of hypotheses. Integrability: $\mathbb{E}h^2 \le 1$. Nondegeneracy: by (A.5), $\zeta_1 = \sigma^2 = 4\mathbb{E}(L)^2\,\mathrm{Var}(L)/(\pi^2|C|^2)$. Because $S \supsetneq C$, a positive fraction of fibers are truncated by the boundary of C, so the truncated length L is not almost-surely constant. Hence, $\mathrm{Var}(L) > 0$, and $\zeta_1 > 0$. (See Remark A.1 below.)

Combining $U_n = 2Y/[n(n-1)]$ with (A.9),

$$\sqrt{n}\,(U_n - \theta) \;=\; 2\sqrt{n}\left(\frac{Y}{n(n-1)} - \mu\right) \;\xrightarrow{d}\; N(0, 4\sigma^2),$$

where we used $\mu = \theta/2 = \mathbb{E}(L)^2/(\pi|C|)$. Dividing by 2 yields the claim $\sqrt{n}(Y/[n(n-1)] - \mu) \xrightarrow{d} N(0, \sigma^2)$. □

Remark A.1 (Positivity of σ^2)**.** *The nondegeneracy condition* $\sigma^2 > 0$ *reduces to* $\mathrm{Var}(L) > 0$*. For bounded convex* C *and* S *strictly containing* C*, this always holds: Fibers whose midpoints lie in* S/C *are truncated with a length that genuinely depends on both position and orientation, so* L *has a continuous, nondegenerate distribution on* $[0, l]$*. A useful qualitative bound is* $\mathrm{Var}(L) \leq \mathbb{E}(L)(l - \mathbb{E}(L)) \leq l^2/4$*, obtained by applying* $\mathrm{Var}(X) \leq (b-a)^2/4$ *to the bounded random variable* $L \in [0, l]$*. Thus, the ratio* $\mathrm{Var}(L)/\mathbb{E}(L)^2$ *quantifies the relative magnitude of boundary-induced fluctuation in* L *and is dimensionless; it depends on the geometry of* C *and* S *only through shape ratios. For rectangular* C *and* S*, it can be evaluated in closed form from the results of [8].*

A.3. Proof of Theorem 3.2

The two-length model is a two-sample analog of the equal-length case. Let $\xi_i^{(1)} = (m_i^{(1)}, \theta_i^{(1)})$, $i = 1, \ldots, n_1$, and $\xi_j^{(2)} = (m_j^{(2)}, \theta_j^{(2)})$, $j = 1, \ldots, n_2$, be i.i.d. within each sample and independent across samples. Write L_g for the truncated length of a fiber of original length l_g.

Define three Bernoulli kernels

$$h^{(11)}(\xi_i^{(1)}, \xi_{i'}^{(1)}) = Y_{ii'}^{(11)}, \qquad h^{(22)}(\xi_j^{(2)}, \xi_{j'}^{(2)}) = Y_{jj'}^{(22)}, \qquad h^{(12)}(\xi_i^{(1)}, \xi_j^{(2)}) = Y_{ij}^{(12)}.$$

The total intersection count decomposes as

$$Y \;=\; Y^{(11)} + Y^{(12)} + Y^{(22)}, \tag{A.10}$$

where $Y^{(11)} = \sum_{1 \leq i < i' \leq n_1} Y_{ii'}^{(11)}$, and so forth. By Lemma A.1,

$$p^{(gg')} \;:=\; \mathbb{E}Y_{ij}^{(gg')} \;=\; \frac{2\mathbb{E}(L_g)\mathbb{E}(L_{g'})}{\pi|C|}, \qquad g, g' \in \{1, 2\}. \tag{A.11}$$

Step 1. Expectation. Summing over pairs,

$$\mathbb{E}(Y) \;=\; \binom{n_1}{2} p^{(11)} + \binom{n_2}{2} p^{(22)} + n_1 n_2\, p^{(12)} \;=\; \frac{n_1(n_1-1)\mathbb{E}(L_1)^2 + n_2(n_2-1)\mathbb{E}(L_2)^2 + 2n_1n_2\mathbb{E}(L_1)\mathbb{E}(L_2)}{\pi|C|}.$$

In the asymptotic regime $n_g/n \to \lambda_g$, $n = n_1 + n_2 \to \infty$,

$$\mathbb{E}(Y/n^2) \;\longrightarrow\; \frac{1}{\pi|C|}\big(\lambda_1\mathbb{E}(L_1) + \lambda_2\mathbb{E}(L_2)\big)^2 \;=\; \mu.$$

Step 2. Variance: Systematic enumeration of covariance terms. We expand $\mathrm{Var}(Y) = \sum\sum \mathrm{Cov}(Y_\alpha^{(gg')}, Y_\beta^{(hh')})$ and classify nonzero covariances by the types involved and the pattern of shared fibers. Independence across disjoint fiber sets eliminates all cases in which no fiber is shared, leaving the eight configurations tabulated in Table 5. Each covariance is obtained from Lemma A.1 by conditioning on the shared fiber and using conditional independence of the other fibers given that shared one.

Table 5. Enumeration of the non-zero covariance cases for the two-length mixture model, classified by the types of indicator pairs and the type of the shared fiber. Each covariance value c is obtained from Lemma A.1; the multiplicity counts the number of ordered pairs of indicators in each configuration.

Case	Shared fiber	Covariance value c	Multiplicity (ordered)
$(11) \leftrightarrow (11)$	type-1	$\dfrac{4\mathbb{E}(L_1)^2 \operatorname{Var}(L_1)}{\pi^2\lvert C\rvert^2}$	$n_1(n_1-1)(n_1-2)$
$(22) \leftrightarrow (22)$	type-2	$\dfrac{4\mathbb{E}(L_2)^2 \operatorname{Var}(L_2)}{\pi^2\lvert C\rvert^2}$	$n_2(n_2-1)(n_2-2)$
$(12) \leftrightarrow (12)$	type-1	$\dfrac{4\mathbb{E}(L_2)^2 \operatorname{Var}(L_1)}{\pi^2\lvert C\rvert^2}$	$n_1n_2(n_2-1)$
$(12) \leftrightarrow (12)$	type-2	$\dfrac{4\mathbb{E}(L_1)^2 \operatorname{Var}(L_2)}{\pi^2\lvert C\rvert^2}$	$n_1(n_1-1)n_2$
$(11) \leftrightarrow (12)$	type-1	$\dfrac{4\mathbb{E}(L_1)\mathbb{E}(L_2) \operatorname{Var}(L_1)}{\pi^2\lvert C\rvert^2}$	$2n_1(n_1-1)n_2$
$(22) \leftrightarrow (12)$	type-2	$\dfrac{4\mathbb{E}(L_2)\mathbb{E}(L_1) \operatorname{Var}(L_2)}{\pi^2\lvert C\rvert^2}$	$2n_1n_2(n_2-1)$

We illustrate the derivation of the row $(11) \leftrightarrow (12)$; all other rows follow the same pattern. Consider $\operatorname{Cov}(Y^{(11)}_{ii'}, Y^{(12)}_{ij})$ where a type-1 fiber i is shared by the two indicators. Conditioning on $\xi^{(1)}_i$ and using conditional independence of $\xi^{(1)}_{i'}$ and $\xi^{(2)}_j$,

$$\mathbb{E}\Big[Y^{(11)}_{ii'}Y^{(12)}_{ij}\,\Big|\,\xi^{(1)}_i\Big] \;=\; \frac{2L_{1,i}\mathbb{E}(L_1)}{\pi|C|}\cdot\frac{2L_{1,i}\mathbb{E}(L_2)}{\pi|C|} \;=\; \frac{4L^2_{1,i}\mathbb{E}(L_1)\mathbb{E}(L_2)}{\pi^2|C|^2},$$

so

$$\mathbb{E}[Y^{(11)}_{ii'}Y^{(12)}_{ij}] = \frac{4\mathbb{E}(L_1)\mathbb{E}(L_2)\mathbb{E}(L_1^2)}{\pi^2|C|^2}, \quad \operatorname{Cov} = \frac{4\mathbb{E}(L_1)\mathbb{E}(L_2)(\mathbb{E}(L_1^2)-\mathbb{E}(L_1)^2)}{\pi^2|C|^2} = \frac{4\mathbb{E}(L_1)\mathbb{E}(L_2)\operatorname{Var}(L_1)}{\pi^2|C|^2}.$$

The factor 2 in the multiplicity of row 5 comes from the symmetry $\operatorname{Cov}(Y^{(11)}_{ii'}, Y^{(12)}_{ij}) = \operatorname{Cov}(Y^{(12)}_{ij}, Y^{(11)}_{ii'})$ being counted in both directions in the double-sum (A.6).

Step 3. Leading-order assembly. Adding the variance terms of each of $Y^{(11)}, Y^{(22)}, Y^{(12)}$ (each of order n^2), and the six covariance contributions (each of order n^3), the exact variance is

$$\operatorname{Var}(Y) = \underbrace{\binom{n_1}{2}p^{(11)}(1-p^{(11)}) + \binom{n_2}{2}p^{(22)}(1-p^{(22)}) + n_1n_2p^{(12)}(1-p^{(12)})}_{\text{order } n^2} + \underbrace{\sum_{\text{covariance rows}} (\text{multiplicity})\cdot c}_{\text{order } n^3}. \tag{A.12}$$

Collecting the n^3-order terms and substituting $n_g = \lambda_g n + o(n)$,

$$\operatorname{Var}(Y) \;=\; \frac{4n^3}{\pi^2|C|^2}[\lambda_1\operatorname{Var}(L_1) + \lambda_2\operatorname{Var}(L_2)][\lambda_1\mathbb{E}(L_1) + \lambda_2\mathbb{E}(L_2)]^2 \;+\; O(n^2).$$

A short algebraic verification: The coefficient of n^3 assembles as

$$\lambda_1^3\mathbb{E}(L_1)^2\,\mathrm{Var}(L_1)+\lambda_2^3\mathbb{E}(L_2)^2\,\mathrm{Var}(L_2)+\lambda_1\lambda_2^2\mathbb{E}(L_2)^2\,\mathrm{Var}(L_1)+\lambda_1^2\lambda_2\mathbb{E}(L_1)^2\,\mathrm{Var}(L_2)$$
$$+\ 2\lambda_1^2\lambda_2\mathbb{E}(L_1)\mathbb{E}(L_2)\,\mathrm{Var}(L_1)+2\lambda_1\lambda_2^2\mathbb{E}(L_1)\mathbb{E}(L_2)\,\mathrm{Var}(L_2),$$

which factors neatly as $[\lambda_1\,\mathrm{Var}(L_1)+\lambda_2\,\mathrm{Var}(L_2)][\lambda_1\mathbb{E}(L_1)+\lambda_2\mathbb{E}(L_2)]^2$. Hence,

$$n\cdot\mathrm{Var}\Big(\frac{Y}{n^2}\Big)\ \longrightarrow\ \frac{4[\lambda_1\,\mathrm{Var}(L_1)+\lambda_2\,\mathrm{Var}(L_2)][\lambda_1\mathbb{E}(L_1)+\lambda_2\mathbb{E}(L_2)]^2}{\pi^2|C|^2}\ =\ \sigma^2. \tag{A.13}$$

Remark A.2 (Absence of a direct $\mathrm{Cov}(L_1,L_2)$ term)**.** *The final expression for σ^2 contains $\lambda_1\,\mathrm{Var}(L_1)+\lambda_2\,\mathrm{Var}(L_2)$ but no covariance between L_1 and L_2. The reason is structural: L_1 and L_2 refer to truncated lengths of* different *fibers, which are independent by construction, so $\mathrm{Cov}(L_1,L_2)=0$ trivially. Cross-type effects nevertheless enter σ^2 through the* squared mean factor $(\lambda_1\mathbb{E}(L_1)+\lambda_2\mathbb{E}(L_2))^2$*, which, upon expansion, contributes the cross-mean term $2\lambda_1\lambda_2\mathbb{E}(L_1)\mathbb{E}(L_2)$. This is precisely the contribution of cross-type covariance rows* (11) ↔ (12) *and* (22) ↔ (12) *in the enumeration above: They involve a single shared fiber (of one type) but a partner of the other type, producing $\mathbb{E}(L_1)\mathbb{E}(L_2)$ cross-products rather than $\mathrm{Cov}(L_1,L_2)$ terms.*

Step 4. Asymptotic normality via two-sample U-statistic CLT. The statistic Y is a linear combination of three U-statistics: two one-sample U-statistics ($Y^{(11)}$ on the type-1 sample and $Y^{(22)}$ on the type-2 sample) and one bilinear two-sample U-statistic $Y^{(12)}$ [18, 19]. Under the regime $n_g/n\to\lambda_g\in(0,1)$, the joint Hoeffding projection of $(Y^{(11)},Y^{(12)},Y^{(22)})$ onto the first-order components of the two underlying samples yields a jointly Gaussian limit after appropriate centering and scaling. Consequently, any fixed linear combination, in particular Y/n^2, has a Gaussian limit, as well.

It remains to identify the limiting variance. Combining (A.13) with the fact that the second-order (degenerate) contributions are of smaller order $O(1/n^2)$,

$$\sqrt{n}\Big(\frac{Y}{n^2}-\mu\Big)\ \xrightarrow{d}\ N(0,\sigma^2),$$

where μ,σ^2 are as in Theorem 3.2. Nondegeneracy ($\sigma^2>0$) requires $\lambda_1\,\mathrm{Var}(L_1)+\lambda_2\,\mathrm{Var}(L_2)>0$ and $\lambda_1\mathbb{E}(L_1)+\lambda_2\mathbb{E}(L_2)>0$, both of which hold as soon as *at least one* fiber population has nondegenerate truncated length and $\lambda_1,\lambda_2>0$; in particular, it is implied by the non-degeneracy condition of Theorem 3.1 applied to either population. When $l_1=l_2$, the formula reduces to the equal-length case, as noted in the statement of the theorem.

AIMS Press